JCTC Journal of Chemical Theory and Computation

Article

pubs.acs.org/JCTC

Bending Vibration-Governed Solvation Dynamics of an Excess Electron in Liquid Acetonitrile Revealed by Ab Initio Molecular Dynamics Simulation

Jinxiang Liu,[†] Robert I. Cukier,[‡] and Yuxiang Bu*[,†]

[†]School of Chemistry and Chemical Engineering, Shandong University, Jinan, 250100 Shandong, P. R. China

[‡]Department of Chemistry, Michigan State University, East Lansing, 48824 Michigan, United States

Supporting Information

ABSTRACT: We report an *ab initio* molecular dynamics simulation study of the solvation and dynamics of an excess electron in liquid acetonitrile (ACN). Four families of states are observed: a diffusely solvated state and three ACN core-localized states with monomer core, quasi-dimer (π^*-Rydberg mode) core, and dual-core/dimer core (a coupled dual-core). These core localized states cannot be simply described as the corresponding anions because only a part of the excess electron resides in the core molecule(s). The quasi-dimer core state actually is a mixture that features cooperative excess electron capture by the π^* and Rydberg orbitals of two ACNs. Well-defined dimer anion and solvated electron cavity were not observed in the 5−10 ps simulations, which may be attributed to slow dynamics of the formation of the dimer anion and difficulty of the formation of a cavity in such a fluxional medium. All of the above observed states have near-IR absorptions and thus can be regarded as the solvated electron states but with different structures, which can interpret the experimentally observed IR band. These states undergo continuous conversions via a combination of long-lasting breathing oscillation and core switching, characterized by highly cooperative oscillations of the electron cloud volume and vertical detachment energy. The quasi-dimer core and diffusely solvated states dominate the time evolution, with the monomer core and dual-core/dimer core states occurring occasionally during the breathing and core switching processes, respectively. All these oscillations and core switchings are governed by a combination of the electron-impacted bending vibration of the core ACN molecule(s) and thermal fluctuations.

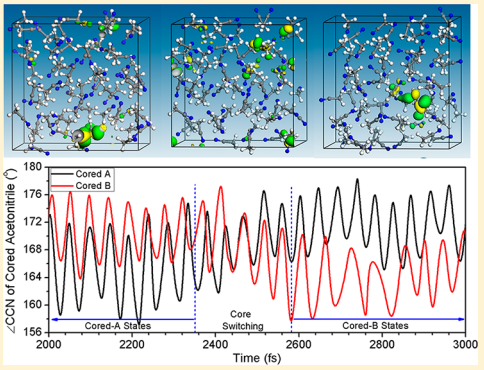

1. INTRODUCTION

Solvation of an excess electron (EE) in condensed matter has attracted widespread interest in physics, chemistry, and biology.[1−8] At present, two different localized forms of an EE in a dielectric medium have been well characterized: the solvated electron and solvent-bound valence anion. A solvated EE occupies a sphere-like cavity (no core) surrounded by solvent molecules such as water, aliphatic alcohols, and saturated hydrocarbons,[9−11] while for the latter, an EE is fully localized on one or two solvent molecules, forming monomer or dimer radical anions.[6,12,13] However, a series of recent studies also reveal other kinds of solvated EE states.[7,14,15] In particular, a dry EE in ionic liquids can localize on positive or negative ions, depending on the LUMO alignments,[7] and, even if the EE is in a localized state, it may span two or more cations, with a noncavity structure.[14] An EE can permeate a local structure in water clusters, forming a large sphere-like hydrogen-bonding network permeating pattern but not a cavity.[15] Despite a wealth of information about the structures and properties of solvated electrons in various molecular clusters, their states and evolution dynamics from solvent effects in fluids or solutions are still poorly understood and are quite different from those in gas phase clusters. A noticeable characteristic in liquids or solutions is that thermal fluctuations and bulk effects lead to a short duration of the localized state (e.g., 50−90 fs in normal water)[16] and continuous state conversions between localized and diffuse states.[6,14] Undoubtedly, the fluctuation-induced rapid evolution dynamics of an EE in fluids gives rise to more complicated solvation structures and evolution mechanism, presenting experimental and theoretical challenges for their characterization. This diversity and complexity of the structures and states of solvated electrons in solution is attributed not only to the structures and properties of solvent molecules but also to the bulk effect, thermodynamic and electronic properties of fluids originating from thermal fluctuations and band structure. In some solvents, bending vibrations predominantly control the trapping, localization, detachment, and even evolution dynamics of an EE.[6,17,18] Thus, a careful exploration of the states and dynamics of EEs in various liquid media is indicated and of fundamental interest.

Received: March 19, 2013
Published: October 15, 2013

   dx.doi.org/10.1021/ct4002174 | J. Chem. Theory Comput. 2013, 9, 4727−4734

Acetonitrile (ACN), a very commonly used solvent and cosolvent,[19−27] also is an appropriate medium for carrying out charge-transfer reactions.[28−35] However, although an ACN molecule has a large dipole moment (3.9−4.3 D), its electron affinities are extremely negative (−2.84 eV/vertical versus −2.22 eV/adiabatic).[13,36−39] Solvating the neutral and anion gives a considerably larger electron affinity of 0.25 eV.[36] These positive values suggest that a covalent monomer anion might be stable in the neat liquid, even though a valence anion does not exist in the gas phase.[13,37−39] There are two potential sites for electron attachment in an ACN molecule, which include the $-CH_3$ outside end using a Rydberg orbital and a $-C\equiv N$ site with two low-lying degenerate π^*-orbitals, although a linear ACN molecule may exhibit a mixed LUMO formed from these orbitals. Thus, three possible solvation structures of an EE in ACN clusters and ACN liquid (*liq*ACN) have been proposed on the basis of experimental and theoretical studies under different conditions: a cavity-like solvated electron, a monomer anion, and a dimer anion surrounded by other ACN molecules as solvent.[8,36,39−43] In particular, recent experimental studies suggest that two electron species (solvated electron versus dimer anion) can coexist in *liq*ACN with an equilibrium on the basis of a statistical analysis of an EE-species ensemble, but detailed time evolution dynamics about the electronic states of the EE species and even an individual EE was not given. In addition, a theoretical simulation about the dynamics of EE attachment to acetonitrile clusters reported the formation dynamics of solvated electron cavity but solvated dimer anion was not observed in 10 ps simulations any clusters.[13b] Although a lot of structural and electronic information about the EE-bound motifs has been acquired experimentally and theoretically, mainly extracted from studies of electron-bound gas phase clusters,[8,13,36−43] a detailed knowledge about an EE in *liq*ACN or ACN solutions is still quite lacking. As reported theoretically and experimentally,[8] in ACN cluster anions, the bound EE is more, and even highly, localized and generally exists as a well-structured solvated electron or as monomer or dimer valence anions. However, in liquids, the same is not true, and the degree of localization of an EE or the real structures (cavity-shaped versus others) of solvated electrons still needs clarification.[44,45]

Microscopic level information about an EE in *liq*ACN is experimentally difficult to obtain due to the ultrafast dynamics and extremely short lifetimes of the solvated electron states. Much of this above-mentioned information is generally acquired from molecular cluster models that do not completely apply to the bulk medium case. In particular, thermal fluctuations of *liq*ACN lead to a variety of electronic states and the complicated dynamics of EEs. In this work, we conduct *ab initio* molecular dynamics (AIMD) simulation studies of an EE injected in *liq*ACN with the aims of identifying the EE states and their time evolution and providing a microscopic level understanding of the interaction of a quasifree electron with *liq*ACN. Our main novel findings are that an EE in *liq*ACN mainly exhibits various solvated EE states including a diffusely solvated state and three families of ACN-core localized states with monomer core, quasi-dimer core, and dual core. Although well-defined cavity-shaped solvated electron and monomer or dimer anions states do not occur in this liquid in our up-to-10 ps AIMD simulations, an AIMD simulation of a prepared solvated dimer anion also shows its possible existence and conversion to the solvated states. These solvated states undergo continuous state conversions via a combination of long-lasting breathing oscillations and core switching that are controlled by electron-impacted bending vibrations of the core ACN molecule and thermal fluctuations of the liquid.

2. SIMULATION METHOD

We performed AIMD simulation studies of an EE injected in *liq*ACN (denoted by EE@*liq*ACN) which consists of 64 ACN molecules in a cubic box of length 17.87 Å on a side (T = 300 K, ρ = 0.764 g/cm^3). The system was allowed to evolve by the classical molecular dynamics simulation for 8 ns in the canonical ensemble. Then, spin unrestricted calculations were carried out in the canonical ensemble for 10 ps after the addition of an EE to the neutral system that was pre-equilibrated for 5 ps using AIMD simulations. Energy and forces are evaluated by Becke, Lee, Yang, and Parr (BLYP) exchange-correlation function[46,47] with a long-range dispersion correlation[48] and a double numerical plus polarization (DNP) basis set.[49] The BLYP function performs reasonably well for describing the properties of liquid acetonitrile (Figures S10−S11).[50] Self-consistent field calculations were done with a convergence criterion of 10^{-6} Hartree on the total energy, and the cutoff of the atomic basis set was 3.5 Å. Gamma points were used to integrate the wave function in reciprocal space. The time step was set 1.0 fs, and the temperature was controlled around 300 K by Nosé-Hoover chain thermostat.[51,52] The spin state of electrons in a single unit cell was changed from singlet to doublet upon the addition of an EE to the equilibrated neutral system, and the total charge of the unit cell was reset to −1. In addition, one additional AIMD simulation (a parallel one with a different initial configuration (Figures S15−S17); another one in a large box containing 100 ACN molecules (Figure S18)) was also carried out for EE@*liq*ACN which supports our conclusions. Also, examinations indicate that the adiabatic assumption is valid for all these AIMD simulations and effects of the self-interaction correction (Figure S19) and the basis sets (Figure S20) are negligible.

3. RESULTS AND DISCUSSION

Upon attachment to the pre-equilibrated neutral *liq*ACN, an EE enters the lowest of a low-lying unoccupied molecular orbital set (Figure 1), distributing over more ACN molecules, as a diffuse state. For each ACN molecule participating in binding the EE, it binds only a part of the EE by a superconjugated π^* orbital consisting of a small fraction of the $-CH_3$ outside Rydberg orbital and the π^* orbital located at its slightly bent CCN fragment (about 174°), as shown in Figure 1a.[53] Inspection of different starting configurations reveals that the vertical electron affinity is 0.37−0.78 eV, indicating that accommodation of an EE by *liq*ACN is thermodynamically favorable, as also supported by the large dipole moment and positive electron affinities (0.25 eV) of a single ACN molecule in its liquid.[36]

One anticipates that the vertically injected EE is metastable or even unstable and that it rapidly relaxes to a stabilized state. Clearly, there are two ways for relaxation of such an EE@*liq*ACN system: intramolecular vibrations and intermolecular reorganization (liquid fluctuation). Such intramolecular vibrations and intermolecular motions or solvent fluctuations not only provide a condition for stabilization but also govern the transient states or structures and subsequent time evolution of the injected EE. As expected, the injected EE gradually stabilizes at an early time of about 40 fs. However, further

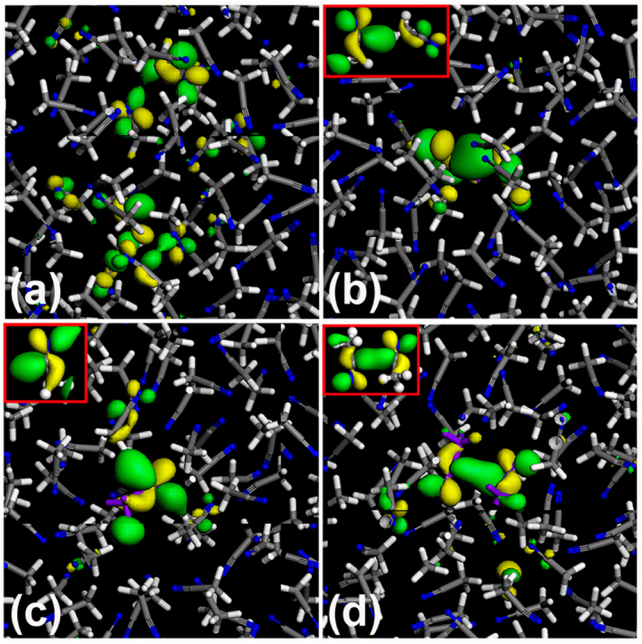

Figure 1. SOMO contours of an EE in *liq*ACN for representative states: (**a**) diffuse state; (**b**) quasi-dimer cored state; (**c**) monomer cored state; and (**d**) dual-cored or dimer-cored state. Surfaces are plotted in a cubic box with an isovalue of 0.03. The insets show a magnification of the localization states. Notably, the monomer core and dual core appear occasionally during the breathing oscillation process and the core switching process, respectively.

observation finds an unexpected phenomenon. A new isomer was first formed as a stabilized structure that is different from the reported cavity-like solvated electron or from the well-defined dimer anion. In this stabilization process, it is not all the ACN molecules that always participate in binding the injected EE or promote its further stabilization. Instead, only one ACN molecule dominates the time evolution. In this initially stabilized structure, two ACN molecules mainly participate in binding the EE. One ACN binds the EE by using its π^* orbital or superconjugated π-like orbital, becoming bent ($\angle$CCN = ~150°). Meanwhile, another ACN interacts with the monomer-bound EE using its $-CH_3$ Rydberg orbital in a dipole-bound form (Figure 1b). This structure is regarded as a quasi-dimer core state for the EE that features a π^*-Rydberg EE-binding mode. All other ACN molecules act as a solvent surrounding the quasi-dimer core. Further examination of the orbital character and spin density distribution of the EE reveals that it becomes localized or quasi-localized in this stabilized snapshot configuration of EE@*liq*ACN; but it is certain that this EE-binding structure cannot be assigned to either a cavity-shaped solvated electron or solvated monomer/dimer anions, as clear from its electronic distribution (about 0.5e over these two main ACN molecules). It actually is a quasi-dimer "quasi-anion" with a fractional negative charge ($ACN^{\delta-}\cdots ACN$), an intermediate-like between the cavity-shaped solvated electron and solvated dimer anion. Unexpectedly, this quasi-dimer core EE state dominates the time evolution. As time progresses, the EE cloud expands to a diffuse state that spreads over several ACN molecules, as suggested by the EE distribution of less than 0.3e over the two core ACN molecules, which is similar to that of the initial state. Interestingly, the spread EE cloud can shrink back to the same core, becoming a localized state. These spreading/shrinking processes can be viewed as systolic and diastolic subprocesses of a breathing motion that is driven and governed by a core ACN molecule. Then, it expands to a slightly diffuse state again. The same events occur in the subsequent time evolution. Clearly, the observed two main states for an EE could be assigned to the diffusely solvated state and solvated quasi-dimer core state. The period of the breathing motion is about 70−100 fs with an average value of about 80 fs, quite similar to that of an isolated ACN anion (ACN^-), although the bending angle ($\angle$CCN = ~130°) of the latter is much smaller than that (~150°) of the former.

Figure 2(a) displays the EE states at three different times in the range of 330−425 fs, which shows the change of the EE states and the corresponding breathing process and period. The

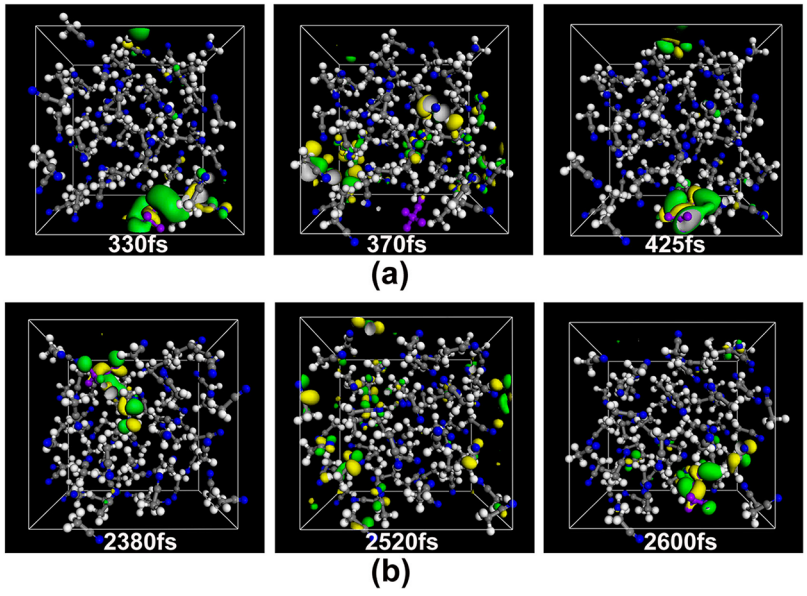

Figure 2. SOMO characters of representative snapshots over two arbitrary time intervals extracted from the AIMD trajectory: (**a**) a breathing period and (**b**) the core-switching shift migration.

dx.doi.org/10.1021/ct4002174 | *J. Chem. Theory Comput.* 2013, 9, 4727−4734

breathing oscillation around the same core can last about 0.6−1.5 ps until the EE gathers around a new core (another ACN) subject to a thermal fluctuation of the liquid. The core switching process occurs through a breathing shift pathway (Figure 2(b)), which describes a transfer step of the EE from one ACN-cored localized state to another. Clearly, this is a novel electron transfer mechanism, distinctly different from that in water or other fluid media. The duration of this core-switching process is about 100−300 fs, 1−4 times the breathing oscillation period (∼80 fs). After core-switching, similar breathing oscillations around the new core continue for some time until the next core is formed.

We characterize the spatial extent of the EE distribution for the breathing oscillation using the enclosed volume and the surface area of the 0.03-isovalued SOMO surface for each snapshot configuration. Generally, when the EE is distributed over many component molecules, its orbital surface exhibits many small lobes and thus has a very small volume encapsulated by the isovalued surfaces of the orbital and a large surface area, whereas when it is localized as a cavity-like state, it exhibits a large lobe (possibly with some additional small lobes) and thus has a large volume and a small surface area. The corresponding time evolution is shown in Figure 3. Unexpectedly, these volumes and areas exhibit a continuous time oscillation, being completely cooperative with the breathing oscillation of the EE distributions mentioned above. They present a strong positive correlation for the surface areas and a strong anticorrelation for the enclosed volumes and thus the localization degree and core-switching migration of the absorbed EE with the bending vibrations of the core ACN molecule(s). That is, the bending vibration of ∠CCN also exhibits a regular oscillation in its time evolution (Figure 3). A small ∠CCN angle of the core ACN corresponds to the closest-packed distribution of the EE with a large volume and a small surface area and thus a localized state, while a large ∠CCN angle corresponds to the slightly diffuse EE distribution with a small volume and a large surface area.

To clarify a possible association of the breathing oscillation with the configuration of *liq*ACN, we further examine geometrical characteristics of the breathing oscillation by analyzing the intramolecular C−C and C−N bond lengths and the distribution of the ∠CCN angle (Figure 4). A distinct difference between an EE-binding core ACN ($ACN^{\delta-}$) and an arbitrary ACN solvent molecule is observed. That is, the bending angular distribution of the core ACN becomes wider, and its peak shifts considerably toward the small angle region, accompanied by a slight lengthening of the C−C and C−N bonds (Figure 4). In general, for a core ACN molecule, its ∠CCN angle oscillates in a range of 151°−173° with an average value of ∼162° and a largest peak value at ∼157°, while a solvent ACN molecule oscillates between 161° and 178° with an average value of ∼174° (Figure 5), which is similar to the neutral *liq*ACN case. The bending and C−C/C−N bond elongation of an ACN molecule enhance its electron-binding ability and thus increases the stability of the EE-binding mode, sometimes with the assistance of a nearby ACN molecule through its dipolar interaction by forming a quasi-dimer core.

Furthermore, besides the above slightly diffuse solvated and solvated quasi-dimer core state, we also observe the monomer core (in π^* mode, $ACN^{\delta-}$) and dual-core (two separated single cores with a fractional negative charge on both core ACN molecules in a π^*/π^* mode, denoted as $ACN^{\delta-}\cdots ACN^{\delta-}$) states in the breathing oscillation process and in the core-switching process (Figure 5), respectively, but occasionally. Note that the well-defined dimer anion and any cavity-shaped solvated electrons, two kinds of the EE-bound modes asserted for the cluster anions, do not occur, at least in our 5−10 ps AIMD simulation. The monomer core can be viewed as a derivative of the above-mentioned quasi-dimer core but with a slightly large intermolecular distance between the two ACN molecules, while the dual-core denotes two separated single cores and can be regarded as a derivative of the dimer core ($\pi^*-\pi^*$ mode); but actually, it is not the dimer anion because the charge of the core unit is only about −0.5. These observations are understandable. Since *liq*ACN is fluxional, due to thermal fluctuations and electron-impacted bending vibrations, the EE-binding motifs are unlikely to possess such well-defined structures.[41,54] Therefore, the monomer core ($ACN^{\delta-}$) and quasi-dimer core ($ACN^{\delta-}$...ACN) can alter-

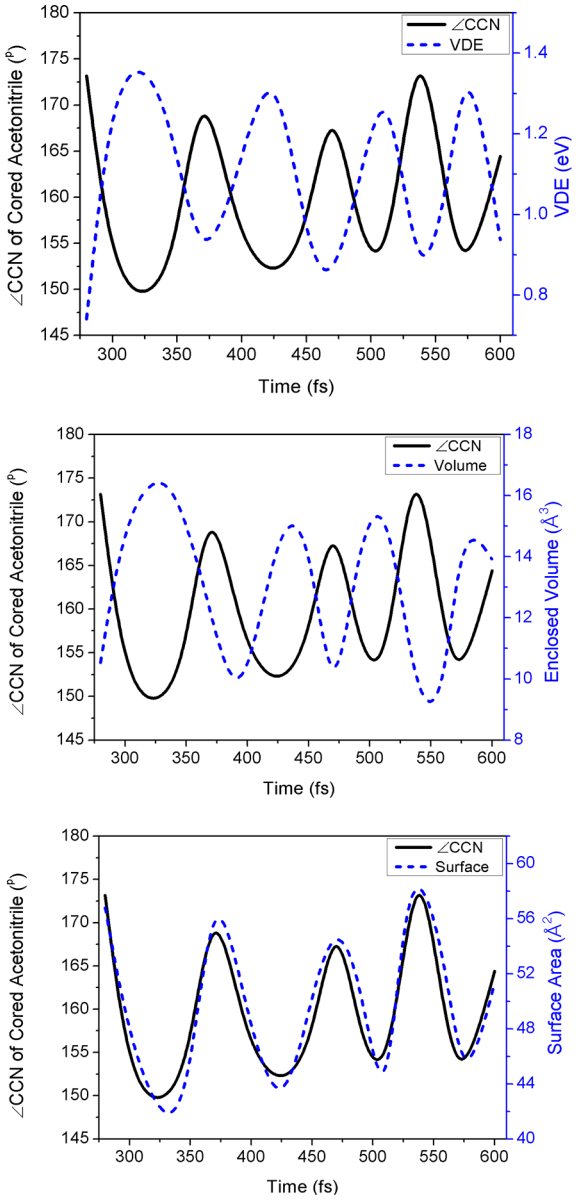

Figure 3. Oscillation behavior of the VDE (top panel/right-axis-scaled), volume (middle panel), and surface area (bottom panel) of the SOMO lobes enclosed by the 0.03-isovalued surface for the EE in *liq*ACN in an arbitrary time period (280−600 fs) and their cooperative relationship with the ∠CCN angle change.

dx.doi.org/10.1021/ct4002174 | J. Chem. Theory Comput. 2013, 9, 4727−4734

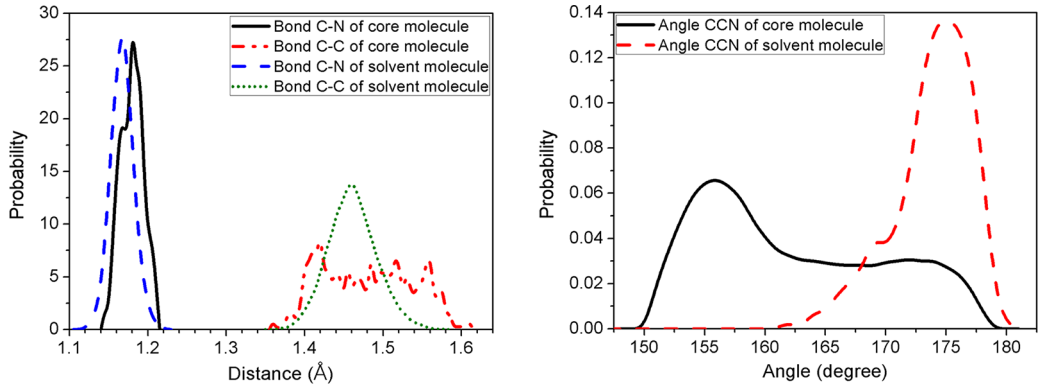

Figure 4. Length distributions of the intramolecular C−C and C−N bonds (left panel) and angular distribution of the intramolecular ∠CCN (right panel) of the core and solvent ACN molecules for the EE@*liq*ACN system.

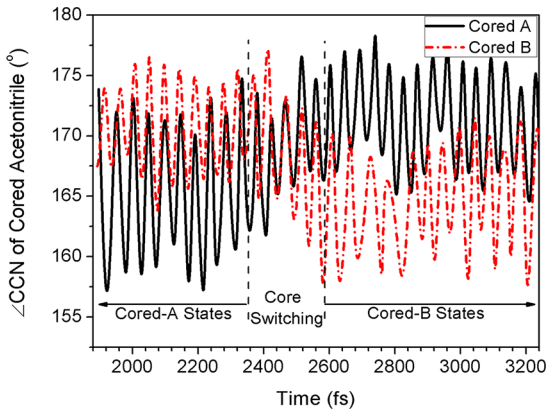

Figure 5. Oscillation of the ∠CCN bending vibration for two arbitrary ACN molecules (**A**/black curve and **B**/red curve) that are the cores, in turn, which bind the EE as localized states. The core-switching occurs at 2360−2580 fs that corresponds to the transfer of the EE from the **A**- to the **B**-cored localized state, mainly experiencing about 4 oscillation periods.

natively appear in the time evolution. For a so-called dimer anion, its electronic structure can be generally expressed as a linear combination of two monomeric contributions. Clearly, this is also true when the two core ACN molecules are separate in the dual core. Thus, the dual core can be formed with high probability during the time evolution, as shown in this AIMD simulation. Furthermore, the formation of a symmetric dimer core requires a symmetric solvent configuration, especially for the first solvation shell. However, one anticipates that such a configuration is unlikely to form in the dynamical process, and thus it is reasonable that the symmetric dimer core does not occur. It should be particularly emphasized that we regard these states as their corresponding cored states instead of their corresponding anions, respectively, because only a part of the EE is localized on the core(s) for each case, as mentioned above.

To evaluate the stability of an EE in *liq*ACN, vertical detachment energies (VDEs) were calculated for selected snapshot configurations along the trajectory, as shown in Figure 3 (first panel/right-axis-scaled). The VDE regularly oscillates in the range of 0.74−1.38 eV, in a highly cooperation manner with the bending oscillation of the ∠CCN of the core ACN and thus with continuous EE breathing oscillations. The slightly diffuse EE states have small VDE values (0.7−0.9 eV), while the localized EE states have slightly large ones (1.1−1.3 eV). This small difference (about 0.6 eV) between the maximum and the minimum value suggests a large mobility for the absorbed EE and also a propensity to escape from *liq*ACN. Note that although an experimental study of negatively charged gas phase clusters, $(ACN)_n^-$ (n = 10−100), clearly assigned two absorbance peaks with VDEs of 0.5−1.0 eV and 2.4−3.0 eV to two well-defined EE-binding motifs (solvated electron versus solvent-bound valence anion), respectively,[8] no reports about VDEs of the relevant species in *liq*ACN have appeared up to now.[36,41] A few results based on different experiment techniques reported inconsistent observations for two EE-binding motifs in *liq*ACN, respectively, monomer and dimer valence anions[40] versus solvated electron and dimer valence anion.[36,41,42] Our calculated VDE oscillations (0.7−1.2 eV for slightly diffuse and monomer cored or quasi-dimer cored states in the breathing process) along the simulation trajectory and VDEs of the ACN anionic clusters seem to support the early asserted solvated electron, monomer and dimer anions, but with a modification of the degree of localization of the EE. In fact, a recent high-level calculation of the VDE (0.358 eV) of a trimer cavity-like solvated electron[13] also implied that even if such a cavity-shaped solvated electron is formed, its VDE should be small (<1.0 eV). This magnitude of the VDE is very close to those of the observed solvated states of the EE reported here which include the diffusely solvated state, solvated quasi-monomer core, solvated quasi-dimer core, and dual core states. Thus, we may infer with confidence that these EE species with low EE-binding energy (e.g., <1.0 eV) should correspond to the diffusely solvated state, and those with middle EE-binding energy (e.g., above 1.0 eV) might simply be regarded as monomer or quasi-dimer core states, depending on if a second ACN molecule interacts in a dipolar manner with the main core. Of course, the species with an EE-binding energy slightly greater than 2.0 eV should correspond to the closely contacted dimer anion, as evidenced by the calculated VDE of a prepared dimer anion in *liq*ACN although it does not occur in our 5−10 ps AIMD simulations for the initial solvation process of an EE. This is understandable from the fluid property that thermal fluctuations are unlikely to greatly reorganize more solvent molecules toward the formation of the solvated electron cavity and also does not favor maintaining the symmetric or quasi-symmetric dimer configuration at its energy minimum for long times, even if it is thermodynamically likely. In short, together with the calculated optical absorption spectra (Figures S23 and S24), these VDEs have further confirmed that all states including the diffusely solvated state, quasi-dimer core

dx.doi.org/10.1021/ct4002174 | *J. Chem. Theory Comput.* 2013, 9, 4727−4734

state, quasi-monomer state, dual core state, and even possible cavity-shaped solvated state observed in the solvation process of an EE belong to the solvated electron states but with different structures.

To further clarify the EE-binding motifs observed here, we calculate the VDEs of the negatively charged gas phase ACN clusters, $(ACN)_n^-$ (n = 2−30), to compare with a previous experimental report.[8] Three well-defined forms (cavity-shaped solvated electron, dimer anion, and quasi-dimer) as cores of the corresponding clusters are considered, and all results including their orbital characteristics and the optical absorption spectra are given in the Supporting Information (Figures S2−S5). As shown in Figure 6, our calculated VDEs of the cavity-shaped

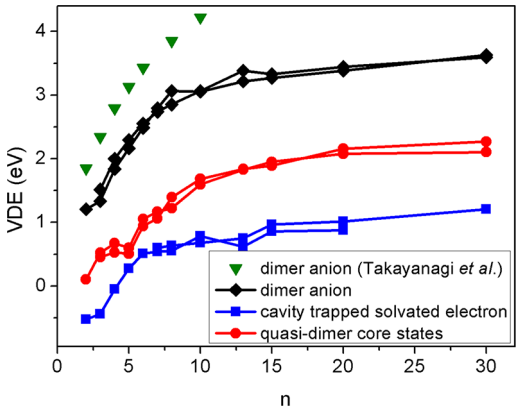

Figure 6. Vertical detachment energies (VDEs) of different EE-binding states of negatively charged ACN clusters, $(ACN)_n^-$ (n = 2−30), as a function of cluster size n calculated at the BLYP/DNP level. The olive down-triangle curve is for the solvent-bound dimer anion form from ref 47 (calculated at the B3LYP/6-31+G(d,p) level of theory).

solvated electron and solvent-bound dimer anion forms agree well with the previous experimental results.[8] The VDEs (0.5−2.0 eV for n = 5−30) of the quasi-dimer form fall in between those corresponding to the cavity-shaped solvated electron and dimer anion but very close to the former. This has fully verified the observed EE-binding states in our AIMD simulations of EE@*liq*ACN all of which belong to the generalized solvated electron states but with different structures. Note that the EE has larger degrees of localization in the cluster model structures compared with those in the liquid case.

In addition, we also examined the possible existence of a cavity-shaped solvated electron and dimer anion by preprepar-ing their structures in *liq*ACN. These two well-defined forms in *liq*ACN are shown in Figures S21 and S22 and have VDEs of 0.86 eV for the cavity-shaped solvated electron and 2.3 eV for the dimer anion. They approximately correspond to the solvated electron and solvent-bound dimer valence anion observed in the photoelectron spectroscopy study of the $(ACN)_n^-$ clusters.[8] Further, our additional AIMD simulations reveal that these two preprepared structures for an EE gradually disappear within about 40 fs for the former to become a diffusely solvated state and about 1150 fs for the latter to become a dual-core state and then a quasi-dimer core state. Clearly, this observation also does not support a cavity-shaped solvated electron. The decay time (∼40 fs) is basically equivalent to the bending vibration period (∼40 fs) of an ACN molecule, indicating that the bending vibration does not favor the formation of a solvation cavity for the EE. However, the long duration (∼100 fs) of the preprepared dimer "anion" form seems to support its existence and a possible association with the dual-core and quasi-dimer core states. In short, these special simulations indicate that well-defined dimer anion and cavity-shaped solvated electrons are not the preferred forms in the solvation process of an EE in *liq*ACN because their formations are kinetically unfavorable, although the former is thermodynamically favorable. Instead, an EE prefers occupancy of a state intermediate between them, the solvent-bound monomer or quasi-dimer core state with a part of the EE over the core molecule(s), exhibiting different forms of the solvated electron state.

4. CONCLUSIONS

In summary, we have shown that for an EE in *liq*ACN, various states including diffusely solvated states and three families of localized states (monomer core ($ACN^{\delta-}$), quasi-dimer core ($ACN^{\delta-}\cdots ACN$), and dual-core ($ACN^{\delta-}\cdots ACN^{\delta-}$)/dimer core states) are observed in the time evolution. Two frequently occurring states, the diffusely solvated and quasi-dimer core states, interconvert through continuous breathing oscillations and core-switching pathways, with the occasional occurrence of monomer core and dual-core/dimer core intermediate states. These core-localized states cannot be simply described as the corresponding anions because only a part of the excess electron resides over the core molecule(s). The quasi-dimer core state actually is a mixed one, featuring a cooperative capture of an excess electron by the π^* and Rydberg orbitals of two ACNs. Although well-defined, cavity-shaped solvated electron and dimer anion were not observed in the fluxional *liq*ACN, AIMD simulations on their prepared structures in *liq*ACN demon-strate they could occur occasionally for the former and after a long time simulation for the latter. All of these observed various states including slightly diffuse state, monomer-core state and solvent-bound quasi-dimer core state, and dual core state should be assigned to the solvated electron states but with different structures which can be also used to account for the experimentally observed near-IR absorption band of an EE in *liq*ACN. These solvated electron states undergo continuous state conversions via a combination of long lasting breathing oscillations and core switching, as also characterized by highly cooperative oscillations of the electron cloud volume and vertical detachment energy. The quasi-dimer core state and diffusely solvated state dominate the entire time evolution, and the monomer core and dual-core/dimer core states occur occasionally during the breathing and the core switching processes, respectively. All these oscillations and core switch-ings are governed by the electron-impacted bending vibration of the core ACN molecule and also by thermal fluctuations. In contrast with cluster-based results in which well-defined solvated electron and solvent-bound dimer anions were reported, our AIMD simulations reveal not only preferential localized states for an EE that are closely associated with the gas phase clustering structures but also the presence of a diffusely solvated state, occurring for about half the trajectory time, that approximately corresponds to a conduction band structure.

■ ASSOCIATED CONTENT

Supporting Information

Calculated data and figures including relaxed potential energy surfaces, optimized geometries, optical absorption spectra, vertical detachment energy, AIMD simulation results, character-istics of LUMO, structural and dynamic properties, reproduc-

tion of the breathing period and core-switching shift migration, additional AIMD simulation results, effects of dispersion interaction and basis set. This material is available free of charge via the Internet at http://pubs.acs.org.

AUTHOR INFORMATION

Corresponding Author

*E-mail: byx@sdu.edu.cn.

Notes

The authors declare no competing financial interest.

ACKNOWLEDGMENTS

This work was supported by NSFC (20633060 and 20973101), NCET, and Independent Innovation Foundation (2009JC020) of Shandong University. A part of the calculations were carried out at Shanghai Supercomputer Center, National Supercomputer Center in Jinan, and High-Performance Supercomputer Center at SDU-Chem.

REFERENCES

(1) Silva, C.; Walhout, P. K.; Yokoyama, K.; Barbara, P. F. Femtosecond Solvation Dynamics of the Hydrated Electron. *Phys. Rev. Lett.* **1998**, *80*, 1086−1089.

(2) Bragg, A. E.; Verlet, J. R. R.; Kammrath, A.; Cheshnovsky, O.; Neumark, D. M. Hydrated Electron Dynamics: From Clusters to Bulk. *Science* **2004**, *306*, 669−671.

(3) Marsalek, O.; Frigato, T.; Vande, V. J.; Bradforth, S. E.; Schmidt, B.; Schütte, C.; Jungwirth, P. Hydrogen Forms in Water by Proton Transfer to a Distorted Electron. *J. Phys. Chem. B* **2009**, *114*, 915−920.

(4) Smyth, M.; Kohanoff, J. Excess Electron Localization in Solvated DNA Bases. *Phys. Rev. Lett.* **2011**, *106*, 238108.

(5) Zurek, E.; Edwards, P. P.; Hoffmann, R. A Molecular Perspective on Lithium−Ammonia Solutions. *Angew. Chem., Int. Ed.* **2009**, *48*, 8198−8232.

(6) Wang, Z. P.; Liu, J. X.; Zhang, M.; Cukier, R. I.; Bu, Y. X. Solvation and Evolution Dynamics of an Excess Electron in Supercritical CO_2. *Phys. Rev. Lett.* **2012**, *108*, 207601.

(7) Margulis, C. J.; et al. Dry Excess Electrons in Room-Temperature Ionic Liquids. *J. Am. Chem. Soc.* **2011**, *133*, 20186−20193.

(8) Mitsui, M.; Ando, N.; Kokubo, S.; Nakajima, A.; Kaya, K. Coexistence of Solvated Electrons and Solvent Valence Anions in Negatively Charged Acetonitrile Clusters, $(CH_3CN)_n^-$ (n = 10−100). *Phys. Rev. Lett.* **2003**, *91*, 153002.

(9) Kevan, L. Solvated Electron Structure in Glassy Matrixes. *Acc. Chem. Res.* **1981**, *14*, 138−145.

(10) Shkrob, I. A.; Sauer, M. C. Electron Trapping by Polar Molecules in Alkane Liquids: Cluster Chemistry in Dilute Solution. *J. Phys. Chem. A* **2005**, *109*, 5754−5769.

(11) Shkrob, I. A.; Myran, C.; Sauer, J. Photostimulated Electron Detrapping and the Two-State Model for Electron Transport in Nonpolar Liquids. *J. Chem. Phys.* **2005**, *122*, 134503.

(12) Shkrob, I. A. Ionic Species in Pulse Radiolysis of Supercritical Carbon Dioxide. 2. Ab Initio Studies on the Structure and Optical Properties of $(CO_2)_n^+$, $(CO_2)_2^-$, and CO_3^- Ions. *J. Phys. Chem. A* **2002**, *106*, 11871−11881.

(13) (a) Takayanagi, T. Ab Initio Study of Small Acetonitrile Cluster Anions. *J. Chem. Phys.* **2005**, *122*, 244307. (b) Takayanagi, T. Theoretical Simulations of Dynamics of Excess Electron Attachment to Acetonitrile Clusters. *Chem. Phys.* **2004**, *302*, 85−93.

(14) Liu, J. X.; Wang, Z. P.; Zhang, M.; Cukier, R. I.; Bu, Y. X. Excess Dielectron in an Ionic Liquid as a Dynamic Bipolaron. *Phys. Rev. Lett.* **2013**, *110*, 107602. Wang, Z.; Zhang, L.; Cukier, R. I.; Bu, Y. X. States and Migration of an Excess Electron in a Pyridinium-Based, Room-Temperature Ionic Liquid: An Ab Initio Molecular Dynamics Simulation Exploration. *Phys. Chem. Chem. Phys.* **2010**, *12*, 1854−1861.

(15) Sommerfeld, T.; Jordan, K. D. Electron Binding Motifs of $(H_2O)_n^-$ Clusters. *J. Am. Chem. Soc.* **2006**, *128*, 5828−5833.

(16) Boero, M.; Parrinello, M.; Terakura, K.; Ikeshoji, T.; Liew, C. C. First-Principles Molecular Dynamics Simulations of a Hydrated Electron in Normal and Supercritical Water. *Phys. Rev. Lett.* **2003**, *90*, 226403.

(17) Narevicius, E.; Moiseyev, N. Trapping of an Electron Due to Molecular Vibrations. *Phys. Rev. Lett.* **2000**, *84*, 1681−1684.

(18) Adams, C. L.; Schneider, H.; Weber, J. M. Vibrational Autodetachment−Intramolecular Vibrational Relaxation Translated into Electronic Motion. *J. Phys. Chem. A* **2010**, *114*, 4017−4030.

(19) Reimers, J. R.; Hall, L. E. The Solvation of Acetonitrile. *J. Am. Chem. Soc.* **1999**, *121*, 3730−3744.

(20) Santoro, F.; Barone, V.; Gustavsson, T.; Improta, R. Solvent Effect on the Singlet Excited-State Lifetimes of Nucleic Acid Bases: A Computational Study of 5-Fluorouracil and Uracil in Acetonitrile and Water. *J. Am. Chem. Soc.* **2006**, *128*, 16312−16322.

(21) Hassinen, A.; Moreels, I.; Nolf, K. D.; Smet, P. F.; Martins, J. C.; Hens, Z. Short-Chain Alcohols Strip x-Type Ligands and Quench the Luminescence of PbSe and CdSe Quantum Dots, Acetonitrile Does Not. *J. Am. Chem. Soc.* **2012**, *134*, 20705−20712.

(22) González, C. M.; Pincock, J. A. Activation Energies for the Singlet Excited State Processes of Substituted Benzenes: Para, Meta, and Ortho Isomers of Methylbenzonitrile and Methylanisole in Acetonitrile. *J. Am. Chem. Soc.* **2004**, *126*, 8870−8871.

(23) Cianci, M.; Tomaszewski, B.; Helliwell, J. R.; Halling, P. J. Crystallographic Analysis of Counterion Effects on Subtilisin Enzymatic Action in Acetonitrile. *J. Am. Chem. Soc.* **2010**, *132*, 2293−2300.

(24) Peryshkov, D. V.; Popov, A. A.; Strauss, S. H. Direct Perfluorination of $K_2B_{12}H_{12}$ in Acetonitrile Occurs at the Gas Bubble−Solution Interface and Is Inhibited by HF. Experimental and DFT Study of Inhibition by Protic Acids and Soft, Polarizable Anions. *J. Am. Chem. Soc.* **2009**, *131*, 18393−18403.

(25) Ellis, W. W.; Raebiger, J. W.; Curtis, C. J.; Bruno, J. W.; DuBois, D. L. Hydricities of BzNADH, $C_5H_5Mo(PMe_3)(CO)_2H$, and $C_5Me_5Mo(PMe_3)(CO)_2H$ in Acetonitrile. *J. Am. Chem. Soc.* **2004**, *126*, 2738−2743.

(26) Stoppa, A.; Hunger, J.; Hefter, G.; Buchner, R. Structure and Dynamics of 1-n-Alkyl-3-n-methylimidazolium Tetrafluoroborate + Acetonitrile Mixtures. *J. Phys. Chem. B* **2012**, *116*, 7509−7521.

(27) Benedetti, E.; Kocsis, L. S.; Brummond, K. M. Synthesis and Photophysical Properties of a Series of Cyclopenta[b]naphthalene Solvatochromic Fluorophores. *J. Am. Chem. Soc.* **2012**, *134*, 12418−12421.

(28) Koch, M.; Rosspeintner, A.; Angulo, G.; Vauthey, E. Bimolecular Photoinduced Electron Transfer in Imidazolium-Based Room-Temperature Ionic Liquids Is Not Faster than in Conventional Solvents. *J. Am. Chem. Soc.* **2012**, *134*, 3729−3736.

(29) Hoff, D. A.; Silva, R.; Rego, L. G. C. Subpicosecond Dynamics of Metal-to-Ligand Charge-Transfer Excited States in Solvated $[Ru(bpy)_3]^{2+}$ Complexes. *J. Phys. Chem. C* **2011**, *115*, 15617−15626.

(30) Zhang, W.; Ji, M.; Sun, Z.; Gaffney, K. J. Dynamics of Solvent-Mediated Electron Localization in Electronically Excited Hexacyanoferrate(III). *J. Am. Chem. Soc.* **2012**, *134*, 2581−2588.

(31) Ehrler, O. T.; Griffin, G. B.; Young, R. M.; Neumark, D. M. Photoinduced Electron Transfer and Solvation in Iodide-Doped Acetonitrile Clusters. *J. Phys. Chem. B* **2008**, *113*, 4031−4037.

(32) Warren, J. J.; Mayer, J. M. Surprisingly Long-Lived Ascorbyl Radicals in Acetonitrile: Concerted Proton−Electron Transfer Reactions and Thermochemistry. *J. Am. Chem. Soc.* **2008**, *130*, 7546−7547.

(33) Chaban, V. V.; Voroshylova, I. V.; Kalugin, O. N.; Prezhdo, O. V. Acetonitrile Boosts Conductivity of Imidazolium Ionic Liquids. *J. Phys. Chem. B* **2012**, *116*, 7719−7727.

(34) Gao, J.; Müller, P.; Wang, M.; Eckhardt, S.; Lauz, M.; Fromm, K. M.; Giese, B. Electron Transfer in Peptides: The Influence of Charged Amino Acids. *Angew. Chem., Int. Ed.* **2011**, *50*, 1926−1930.

(35) Zhu, X. Q.; Zhang, M. T.; Yu, A.; Wang, C. H.; Cheng, J. P. Hydride, Hydrogen Atom, Proton, and Electron Transfer Driving Forces of Various Five-Membered Heterocyclic Organic Hydrides and Their Reaction Intermediates in Acetonitrile. *J. Am. Chem. Soc.* **2008**, *130*, 2501−2516.
(36) Xia, C.; Peon, J.; Kohler, B. Femtosecond Electron Ejection in Liquid Acetonitrile: Evidence for Cavity Electrons and Solvent Anions. *J. Chem. Phys.* **2002**, *117*, 8855−8866.
(37) Steiner, P. A.; Gordy, W. Precision Measurement of Dipole Moments and Other Spectral Constants of Normal and Deuterated Methyl Fluoride and Methyl Cyanide. *J. Mol. Spectrosc.* **1966**, *21*, 291−301.
(38) Gutsev, G. L.; Sobolewski, A. L.; Adamowicz, L. A Theoretical Study on the Structure of Acetonitrile (CH_3CN) and Its Anion CH_3CN^-. *Chem. Phys.* **1995**, *196*, 1−11.
(39) Shkrob, I. A.; Takeda, K.; Williams, F. Electron Localization in Solid Acetonitrile. *J. Phys. Chem. A* **2002**, *106*, 9132−9144.
(40) Bell, I. P.; Rodgers, M. A. J.; Burrows, H. D. Kinetic and Thermodynamic Character of Reducing Species Produced on Pulse Radiolysis of Acetonitrile. *J. Chem. Soc., Faraday Trans. 1* **1977**, *73*, 315−326.
(41) Shkrob, I. A.; Sauer, M. C. Electron Localization in Liquid Acetonitrile. *J. Phys. Chem. A* **2002**, *106*, 9120−9131.
(42) (a) Doan, S. C.; Schwartz, B. J. Ultrafast Studies of Excess Electrons in Liquid Acetonitrile: Revisiting the Solvated Electron/Solvent Dimer Anion Equilibrium. *J. Phys. Chem. B* **2013**, *117*, 4216−4221. (b) Doan, S. C.; Schwartz, B. J. Nature of Excess Electrons in Polar Fluids: Anion-Solvated Electron Equilibrium and Polarized Hole-Burning in Liquid Acetonitrile. *J. Phys. Chem. Lett.* **2013**, *4*, 1471−1476.
(43) Becke, A. D. Density-Functional Exchange-Energy Approximation with Correct Asymptotic Behavior. *Phys. Rev. A* **1988**, *38*, 3098−3100.
(44) Uhlig, F.; Marsalek, O.; Jungwirth, P. Unraveling the Complex Nature of the Hydrated Electron. *J. Phys. Chem. Lett.* **2012**, *3*, 3071−3075.
(45) Larsen, R. E.; Glover, W. J.; Schwartz, B. J. Does the Hydrated Electron Occupy a Cavity? *Science* **2010**, *329*, 65−69.
(46) Lee, C.; Yang, W.; Parr, R. G. Development of the Colle-Salvetti Correlation-Energy Formula into a Functional of the Electron Density. *Phys. Rev. B* **1988**, *37*, 785−789.
(47) Takayanagi, T.; Hoshino, T.; Takahashi, K. Electronic Structure Calculations of Acetonitrile Cluster Anions: Stabilization Mechanism of Molecular Radical Anions by Solvation. *Chem. Phys.* **2006**, *324*, 679−688.
(48) Grimme, S. Semiempirical GGA-Type Density Functional Constructed with a Long-Range Dispersion Correction. *J. Comput. Chem.* **2006**, *27*, 1787−1799.
(49) Delley, B. Analytic Energy Derivatives in the Numerical Local-Density-Functional Approach. *J. Chem. Phys.* **1991**, *94*, 7245−7250.
(50) VandeVondele, J.; Lynden-Bell, R.; Meijer, E. J.; Sprik, M. Density Functional Theory Study of Tetrathiafulvalene and Thianthrene in Acetonitrile: Structure, Dynamics, and Redox Properties. *J. Phys. Chem. B* **2005**, *110*, 3614−3623.
(51) Hoover, W. G. Canonical Eynamics: Equilibrium Phase-Space Distributions. *Phys. Rev. A* **1985**, *31*, 1695−1697.
(52) Tuckerman, M. E.; Liu, Y.; Ciccotti, G.; Martyna, G. J. Non-Hamiltonian Molecular Dynamics: Generalizing Hamiltonian Phase Space Principles to Non-Hamiltonian Systems. *J. Chem. Phys.* **2001**, *115*, 1678−1702.
(53) In *liq*ACN, each ACN molecule is bent with a ∠CCN angle of ∼164−179° (an average value of 171°), which is similar to the CO_2 case in the supercritical state [ref 6], but its polarity is slightly smaller than that of the linear gas phase ACN molecule. In addition, bending also reduces the degree of superconjugation between the −C≡N π^* orbital and the −C−H Rydberg orbital with an increase of the −C≡N π^* orbital composition and a decrease of the −C−H Rydberg orbital in the LUMO, in going from the linear to bent structure. That is, bending changes the −C≡N π^* orbital to a dominant contributor in the LUMO of an ACN.
(54) Shkrob, I. A.; Sauer, M. C. Metastable Electrons, High-Mobility Solvent Anions, and Charge Transfer Reactions in Supercritical Carbon Dioxide. *J. Phys. Chem. B* **2001**, *105*, 4520−4530.